Proceedings of the ASME 2019
Verification and Validation Symposium
VVS2019
May 15-17, 2019, Las Vegas, NV, USA

VVS2019-5112

BAYESIAN APPROACH TO ESTIMATING FIREBALL PARAMETERS FROM REMOTE SENSING DATA

Derek E. Armstrong
Verification and Analysis
X-Computational Physics
Los Alamos National Laboratory
Los Alamos, New Mexico 87545
Email: dearmstr@lanl.gov

ABSTRACT

Remote sensors in the infrared region can be used to study the progression of fireballs generated from experiments involving high explosives (HE). Developing an improved understanding of HE fireballs can be used to validate and improve computational physics codes that simulate such events. In this paper, Bayesian approaches are studied to estimate time-dependent optimal fireball parameters and their uncertainties using Fourier transform infrared (FTIR) spectroscopy. The optical signal measured by an FTIR sensor provides information on the fireball due to thermal emission, particulate emission/absorption, and HE gas product emission/absorption from the fireball. FTIR sensors have the advantage of being able to capture and measure the radiance in a large part of the infrared spectrum. The parameters to be estimated from the fireball include temperature and size, soot quantity, gas species concentrations (e.g., H_2O, CO_2, CO), and information on the presence of metals. In general, this inverse optimization problem is difficult due to the estimated quantities being correlated, the low spectral resolution of the FTIR sensor, and the intervening atmosphere absorbing the radiation emitted from the fireball. Bayesian calibration and Bayesian model averaging are applied to address these difficulties and to quantify the uncertainty in the estimated optimal parameter values. The fireball parameter settings are evaluated by the fit of a simplified spectral model to FTIR data. The overall problem will be presented together with a description of the Bayesian approaches. In this paper, the Bayesian approaches are applied to artificially generated FTIR data to illustrate the approach.

NOMENCLATURE

τ_{atm} atmospheric transmission
BIC Bayesian information criterion
BMA Bayesian model averaging
$B(\nu,T)$ blackbody function
d experimental data
ε emissivity
FTIR Fourier Transform Infrared
ξ gas concentrations
$\sigma(\nu,T)$ gas cross sections
HE high explosives
L likelihood function
MCMC Markov chain Monte Carlo
$m(\nu)$ model of at-sensor radiance
$\boldsymbol{\theta}$ fireball parameters
l sensor line-shape
κ soot absorption coefficient
T fireball temperature
ω unknown Gaussian variance
ν wavenumber
w fireball width

INTRODUCTION

The purpose of this work is to investigate Bayesian methods for the problem of estimating high explosive (HE) fireball parameters from remote sensing data. A particular interest is in using FTIR (Fourier Transform Infrared) spectroscopy to remotely monitor infrared emissions from experiments involving HE and

estimate the fireball parameters as a function of time. The fireball parameters of interest to this work is temperature, fireball size, soot quantity, concentration of the gases H_20, CO_2, and CO, and the presence of specific metals. Other gases in the fireball, such as CH_4, can also impact the fireball emissions, but they are not considered in this paper. The interest in understanding fireball dynamics is to help with the verification and validation of computational computer codes that model such HE events.

The advantage to using Bayesian approaches for this problem is to quantify the uncertainty in the estimated fireball parameters. This paper will investigate the use of two Bayesian approaches for quantifying the uncertainty in the estimated fireball parameters. Traditional optimization methods can be used to find optimal or near-optimal parameter settings for a forward model of experimental data. These methods by themselves do not compare and consider different parameter settings in order to develop confidence assessments in the found parameter settings. Bayesian or probabilistic methods have the advantage of considering many model parameter settings to provide more information on parameter settings that provide quality fits to data. In this paper, Bayesian calibration and Bayesian model averaging (BMA) are used to address this fireball parameter estimation problem. The Bayesian calibration method will assume an error term that is a multivariate Gaussian with an inverse Gamma prior on the unknown variance. The posterior distribution will be estimated by computing a forward model and comparing it to the data for a large grid of parameter settings and, in future work, by the use of Markov chain Monte Carlo (MCMC) methods. The BMA method will be based on using the Bayesian information criterion (BIC) to estimate posterior model probabilities. Both of these approaches allow for the computation of marginal probability distributions for the fireball parameters.

Previous work on estimating fireball parameters from remote sensing data includes research by Gross [1], [2] and Slagle [3]. In the work by Gross, a spectral model was used for fireball emissions that consisted of seven parameters (includes gas HCl). Gross [1] assumed Gaussian noise (with an estimated standard deviation) and constructed confidence intervals for the fireball parameters of the nonlinear regression problem. The research presented here, in contrast, is using BMA to estimate model and marginal probability distributions for the fireball parameters. Also, for the Bayesian calibration in this paper, the variance of the error term is assumed unknown (except it follows an inverse Gamma distribution) and is estimated during the calibration. The research by Slagle [3] used a five parameter (size, temperature, soot quantity, H_2O concentration, and CO_2 concentration) model to characterize fireball emissions. Slagle [3] estimates the five parameters by using selected sensor bands and does not attempt to model the full fireball spectra. For example, two wavenumber bands, centered at 2580 cm^{-1} and 4535 cm^{-1}, were used to estimate temperature. A total of five bands were selected to estimate the five parameters. The work of Slagle [3] demonstrates that acceptable estimates of fireball parameters could be obtained without modeling the full fireball spectrum.

MODELING SPECTRA AND FTIR SENSORS

The radiance emitted from a fireball can be monitored in the infrared region by a remote sensor and used to identify characteristics of the fireball. The fireball will emit radiation based on its temperature, particulate absorption (soot), the gases that make up the fireball, and the presence of any metals (in the form of flying fragments). The different gases of the fireball have different absorption lines and cross sections that allow for the gas concentrations to be estimated from remote sensing data. The presence of specific metals can be determined by their emissivity signatures (emissivity as a function of wavenumber). Due to the smoothly varying nature of solid emission as a function of wavenumber, the detection of metal fragments in the fireball is a difficult problem and Bayesian approaches are needed for uncertainty quantification. The intervening atmosphere between the fireball and sensor will absorb radiation emitted by the fireball. The atmospheric transmission must be modeled in order to estimate fireball parameters.

FTIR sensors are well-suited to monitoring experiments with HE since they can observe radiation over a wide range of the infrared spectrum (e.g., one experiment covered wavelengths from 1 to 15 microns). A disadvantage to FTIR data is that it is single pixel and can have low time resolution. The fact that FTIR data is single pixel means that the data recorded is spatially integrated. For the work in this paper, the FTIR sensor is assumed to have 32 cm^{-1} resolution (results in an approximate 16 cm^{-1} width for wavenumber bands) covering wavenumbers 2000 cm^{-1} to 5000 cm^{-1}. In a recent experiment, such a configuration also consisted of a time resolution of about 0.01 seconds. The time resolution is not of concern in this paper since the focus is on fitting spectra individually. Also, the work in this paper will be restricted to applying the fireball modeling to artificially generated spectra. An example of an artificial FTIR spectrum is given in Fig.1. The artificial spectrum in Fig.1 consists of the following parameter settings: fireball length of 400 cm, temperature of 1500K, soot concentration of 7.5E-05 cm^{-1}, and H_2O, CO_2, and CO concentrations of 9E17, 2E18, and 3E18 molecules/cm^3, respectively [4]. Gaussian noise with a standard deviation of three percent was also added to the artificial spectrum.

The monochromatic fireball radiance can be modeled by Eqn. (1) when metal fragments are not present or their contribution to the total radiance is minimal. Research by Gross [1] indicates that using a single temperature to model fireball spectrum is adequate for FTIR data:

$$m_1(\nu) = w^2 \varepsilon_{FB}(\nu) B(\nu, T) \tau_{atm}(\nu) \tag{1}$$

where the fireball emissivity is given by

$$\varepsilon_{FB}(\nu) = 1 - exp(-w(\kappa + \sum_i \sigma_i(\nu, T)\xi_i)). \tag{2}$$

Including emission from flying metal fragments leaving the fireball, the fireball model spectrum is:

$$m_2(\nu) = w^2 \varepsilon_{FB}(\nu) B(\nu, T) \tau_{atm}(\nu) + \sum_i c_i \varepsilon_i B(\nu, T_i) \tau_{atm}(\nu) \quad (3)$$

where the second term in Eqn. (3) is the emission from metal fragments (indexed by i for different metals in the fireball) and c_i is the area term for the corresponding metal.

The exponential term in Eqn. (2) represents the transmission of the fireball. The transmission of the fireball will depend on the absorption cross sections σ_i, in units of cm^2/molecule, for each gas (H_2O, CO_2, CO), the soot absorption coefficient κ in units of cm^{-1}, and the concentration ξ_i of each gas i in units of molecules/cm^3. Due to the hot temperature of the fireball, the emission of the environment surrounding the fireball and being observed by the FTIR sensor can be ignored since its contribution to the at-sensor radiance is minimal. The cross sections are due to the absorption lines of the different gases being considered. There are millions of absorption lines in these gases which makes the modeling process computationally challenging. Also, it is very important to appropriately model the sensor response to the observed radiance. The sensor response is also referred to as the sensor line-shape. Incorporating the line-shape l, the at-sensor radiance for band i, centered at wavenumber ν_i, is given by

$$m_s(\nu_i) = \int_0^\infty l(\nu - \nu_i) m(\nu) d\nu. \quad (4)$$

where $m(\nu)$ in Eqn. (4) can be $m_1(\nu)$ or $m_2(\nu)$ depending on presence of metal fragments or not.

In the case of the FTIR sensor, the line-shape depends on the characteristics of the sensor and the manner in which the data is processed. To obtain spectra from a FTIR interferogram, the Fourier transform is applied to the raw sensor data after the application of an apodization function. The apodization function is necessary to obtain a more accurate representation of the observed radiance. In this paper, a triangular apodization function is used and the resultant line-shape for the FTIR sensor is a sinc function. The width of the sinc function for the line-shape depends on the resolution of the FTIR sensor.

BAYESIAN METHODOLOGY USED IN THIS PAPER

Several approaches can be applied to the FTIR data to estimate fireball parameters. Optimization techniques can be applied to find optimal, or near-optimal, parameter settings for model $m_i(\nu)$, i = 1 or 2, that best fit the FTIR data. Optimization approaches do not provide information on uncertainty in the found parameter settings. Also, they do not attempt to quantify the ranges of parameter settings that allow the model $m_i(\nu)$ to adequately represent the data.

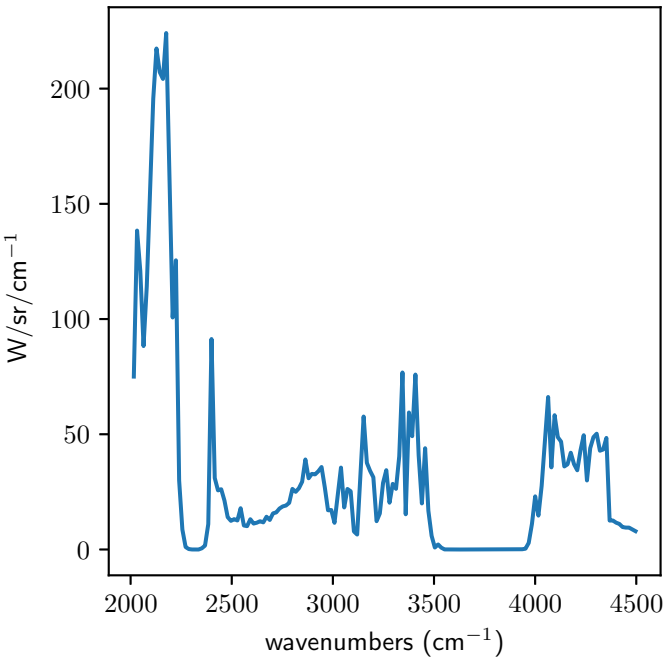

FIGURE 1. ARTIFICIAL SPECTRUM FOR FTIR

Two Bayesian approaches are considered in the paper. The first method consists of using the Bayesian information criterion (BIC) [5] to estimate posterior model probabilities through BMA [6]. The work by Burr et al. [5] investigated several variations of the BIC, as described in the work of Neath and Cavanaugh [7], to estimate model probabilities. The second method consists of a Bayesian calibration, where a Gaussian likelihood is used in conjunction with an inverse Gamma distribution for the unknown Gaussian variance.

The BIC is an asymptotic (large sample) approximation to a logarithmic transformation of the full Bayesian posterior probability. The approximation is based off of removing terms in a Taylor series approximation of the logarithmic transformation that are negligible or independent of the model specifics. The BIC can be used to estimate the Bayesian posterior probability for a model M, according to

$$P(M|d) = e^{-BIC/2} \quad (5)$$

where the BIC is

$$BIC = kln(n) - 2ln(L_{max}). \quad (6)$$

In Eqn. (5) and (6), k is the number of model parameters, n is the number of wavenumber bands, and L_{max} is the maximum value of the likelihood function. For the results in this paper, an

independent multivariate Gaussian is assumed for the likelihood when performing BMA. The BIC is based off of using a Taylor series approximation to the logarithm of the Bayesian posterior probability, where the Taylor series is centered around the maximum value of the likelihood function. As an illustration, consider a linear regression problem, then the least squares solution is analytic and provides the maximum value of the likelihood function. In this paper, the BIC will be used to estimate model probabilities M for fireball models involving both $m_1(\nu)$. In the case of fireball model $m_1(\nu)$, which does not include metal fragments, the models M in Eqn. (6) will be parameterized by values for gas concentrations of H_2O, CO_2, and CO. The maximum likelihood of Eqn. (6) is obtained by finding optimal values for the fireball size, temperature, and soot concentration for fixed model M (gas concentrations). The model M is constructed in this way for Bayesian model averaging since the fireball size, temperature, and soot concentration impact the magnitude of the fireball and can be found readily and accurately for fixed gas concentration values. Performing the analysis in this way allows for quicker computations since the dimensionality of the problem, in some sense, has been reduced by a factor of 2. For the fireball model with metal fragment emission $m_2(\nu)$, the computation of the BIC and BMA is more traditional. Since the number of possibilities for the metals is quite large (10s to maybe even 100), the BIC can be used to compute model probabilities for models M that are defined by a set of metals. For example, a model M could represent the presence of aluminum and steel and the corresponding maximum likelihood in Eqn. (6) is obtained by optimizing the remaining parameters (fireball size, temperature, etc.) given the presence of aluminum and steel. This type of use of BIC and BMA was used in [5]. The BIC can be computed for a large number of models M defined by the presence of different metals and then BMA can be used to compute probabilities a specific metal being present in the fireball by computing the following:

$$P(\text{metal } i) = \sum_{M \text{ contains } i} P(M|d). \tag{7}$$

For the results in the next section, the BIC will be computed for the fireball model $m_1(\nu)$. Therefore, those results will provide an estimate of the posterior probability for the gas concentrations in the fireball. Future work will investigate the use of the BIC to estimate the probability of specific metals being present in the fireball as described for model $m_2(\nu)$. The BIC and resultant model probability is computed for a large number of models $m_1(\nu)$ and then BMA can be used to estimate marginal probabilities for the gas concentrations. Similar to Eqn. (7) above, probabilities for the gas concentrations can be computed with the following:

$$P(\theta_l < \theta < \theta_u) = \sum_{M_i \in M_I} P(M_i|d). \tag{8}$$

where M_I is all models with $\theta_l < \theta < \theta_u$ and θ represents one of the gas concentrations.

The Bayesian model averaging method just described will be compared with a Bayesian calibration method. The Bayesian calibration method assumes a likelihood function that is an independent multivariate Gaussian with a common percent variance. Therefore, the model assumes that the variance is a common percentage of the computed radiance values so that larger radiance values have larger variances. The variance represents the error in sensor measurement and due to missing model terms. The variance for the likelihood will be denoted by ω. The likelihood for this Bayesian calibration is given by

$$p(d|\boldsymbol{\theta}, \omega) = \left(\sqrt{2\pi\omega}\right)^{-n/2} exp^{-\chi^2} \tag{9}$$

where $\boldsymbol{\theta}$ is the set of model parameters and

$$\chi^2 = \sum_{j=1}^{n} \frac{(d_j - m(\nu_j, \boldsymbol{\theta}))^2}{2m(\nu_j, \boldsymbol{\theta})^2 \omega}. \tag{10}$$

In the above equation, d_j and $m(\nu_j, \boldsymbol{\theta})$ are the data and model radiance values at wavenumber band j, and n is the number of data points (spectral wavenumber bands). For Eqn. (10), the dependence of the model on the model parameters $\boldsymbol{\theta}$ is given explicitly. An inverse Gamma distribution will be used for the prior distribution of the unknown percent variance ω. The inverse Gamma distribution has two parameters α and r. The prior density function for ω is

$$p(\omega) = \frac{\alpha^r}{\Gamma(r)} \omega^{-r-1} exp^{-\alpha/\omega}. \tag{11}$$

The parameters will be given a uniform prior over the hypercube A. Let $I_A(\boldsymbol{\theta})$ be the indicator function for hypercube A (i.e., $I_A(\boldsymbol{\theta})$ is equal to one when $\boldsymbol{\theta} \in A$ and zero otherwise). The posterior satisfies the following:

$$p(\boldsymbol{\theta}, \omega|d) \propto p(d|\boldsymbol{\theta}, \omega) p(\omega) I_A(\boldsymbol{\theta}). \tag{12}$$

By rearranging and simplifying, the conditional posterior for ω, given $\boldsymbol{\theta}$ and d satisfies

$$p(\omega|\boldsymbol{\theta}, d) \propto \omega^{-n/2-r-1} exp((-\chi^2\omega - \alpha)/\omega). \tag{13}$$

Therefore, the conditional posterior is an inverse Gamma with the parameters

$$\tilde{r} = \frac{n}{2} + r \text{ and } \tilde{\alpha} = \sum_{j=1}^{n} \left(\frac{(d_j - m_j(\nu_j, \boldsymbol{\theta}))^2}{2m_j(\nu_j, \boldsymbol{\theta})^2} \right) + \alpha. \qquad (14)$$

The hyperparameters α and r will be selected with the help of an estimated value for ω obtained from a coarse fit to the data. Let $\hat{\omega}$ represent this estimated variance. The inverse Gamma distribution has expected value $\alpha(r-1)^{-1}$. Therefore, α and r will be selected so that $\alpha = (r-1)\hat{\omega}$. The inverse Gamma has a finite mean for $r > 1$ and it has finite variance for $r > 2$. Since it is desired to have a prior that is not strongly informative, r will be chosen to be between 1 and 2. For the results in this paper, a value of $r = 1.5$ is used which implies that $\alpha = 0.5\hat{\omega}$. The estimated value for $\hat{\omega}$ was determined to be around 0.05^2, which implies that the estimated standard deviation of the model to the data is around 5%. The posterior will be integrated to obtain marginal density functions for the parameters (including variance ω). To integrate the posterior, a uniform grid will be constructed over the hypercube A and values for ω, which effectively reduces the continuous parameter space domain to a discrete domain. The fact that the conditional posterior of ω is an inverse Gamma is used to reduce the number of model computations. Future work will investigate the use of MCMC (including the use of Gibbs sampling) to estimate the parameters.

RESULTS

The BMA and Bayesian calibration methods were applied to two artificial spectra. The first set of results given in this section is for the artificial spectrum of Fig. 1. The artificial data for that spectrum was constructed with the following model parameters: temperature of 1500K, width of 400 cm, soot quantity of 7.5E-05 cm^{-1}, and H_2O, CO_2, and CO concentrations of 9E17, 2E18, and 3E18 molecules/cm^3, respectively. Additionally, a three percent error term was added to the artificial spectrum.

BMA and Bayesian calibration were applied to the artificial spectrum of Fig. 1 assuming temperature and width were known. In the case of BMA, this means that the maximum likelihood for the model (gas concentrations) probability (see Eqn. (6)) was obtained by optimizing over the soot concentration. This was done to limit the number of computations of the spectral model $m(\nu)$. The spectral model is computed with a wavenumber resolution of 0.001 cm^{-1} and the line-shape is used to convolve the high-resolution model to the sensor wavenumbers. Both BMA and Bayesian calibration used a temperature of 1510 K and a width of 390 cm. Different values for temperature and width were used to determine the effectiveness of the approach when the given parameters are not known exactly. The BMA approach was obtained by computing the maximum likelihood for about 15,000 models (about 25 grid values for each of the three gas concentrations). The maximum likelihood was obtained for each of these 15,000 models by an optimization routine for varying the soot. The optimization routine used a linear fit and was computationally efficient. The computations for Bayesian calibration used a discrete grid consisting of more than 390,000 parameter settings (approximately 25 grid values for each of the four parameters). The marginal distributions for the BMA approach and Bayesian calibration are given in Fig. 2 and Fig. 3, respectively. In this paper, the distributions for the gases are unscaled in the figures. This is done since, in many cases, the gas concentrations vary by orders of magnitude and it is desired to have the distributions of all gases in a single plot.

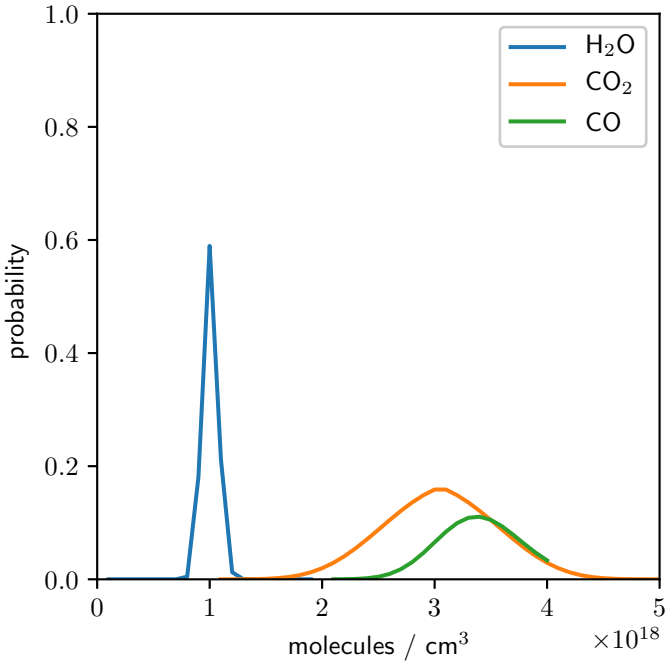

FIGURE 2. BMA RESULTS FOR GAS CONCENTRATIONS

The results in Fig. 2 and Fig. 3 demonstrate that the Bayesian calibration is more accurate in determining the appropriate gas concentrations of CO_2 and CO. Both methods obtain accurate estimates of the H_2O concentration of 9E17 molecules/cm^3. Even though BMA returns worse results it is still a good option to explore further since it will require fewer computations as compared to Bayesian calibration. The Bayesian calibration approach relies on estimating the full multi-dimensional posterior probability. The BMA approach uses approximations based on the maximum likelihood and by choosing the correct parameters to optimize over, the problem of determining the maximum likelihood will not be computationally intensive.

Figure 4 provides the marginal distribution for the soot quantity obtained from the Bayesian calibration approach. Figure 5 gives the distribution obtained from Bayesian calibration for the unknown model variance. Bayesian calibration finds an accurate estimate of the soot quantity (6.5E-05 vs 7.5E-05 cm^{-1}). Interestingly, the standard deviation found by Bayesian calibration was approximately six percent, whereas the prior mean was five percent and the actual artificial spectrum used nine percent. The discrepancy could be due to not having enough samples for the

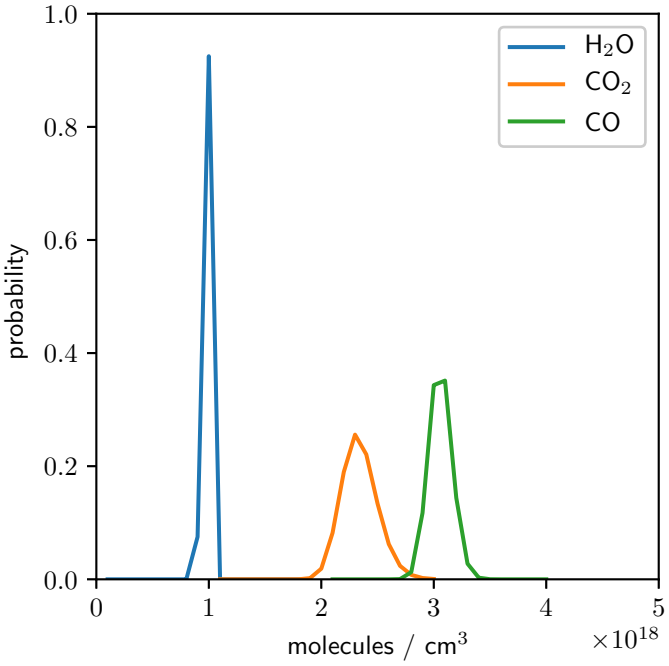

FIGURE 3. BAYESIAN CALIB. FOR GAS CONCENTRATIONS

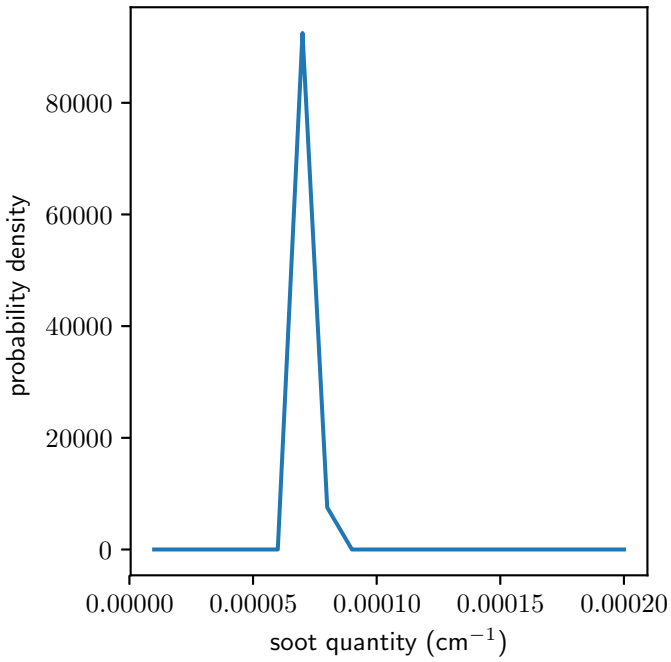

FIGURE 4. BAYESIAN CALIB. FOR SOOT QUANTITY

Bayesian posterior calculation or due to the model assuming a slightly incorrect temperature and width.

The Bayesian approaches were applied to another artificial FTIR spectrum. This second artificial spectrum was constructed with the following parameters: temperature of 1195K, width of 310 cm, soot quantity of 1E-03, and H_2O, CO_2, and CO concentrations of 6E17, 1.7E18, and 1.2E17 molecules/cm^3, respectively. For this data spectrum, all six parameters were considered in the Bayesian approaches. For BMA, the models were specified by the gas concentrations and the maximum likelihood used in Eqn. (6) was obtained by optimizing over the remaining three parameters of temperature, size, and soot concentration. Again, 15,000 models were considered for BMA and for each model the maximum likelihood was determined by optimizing over temperature, size, and soot quantity. Approximately 1,000,000 settings were considered for the Bayesian calibration method with six parameters (10 grid values per parameter). For this second artificial spectrum, the results between BMA and Bayesian calibration are much closer.

Next steps in this work is to use MCMC methods to sample from the Bayesian posterior and to compare those results to BMA. The BMA method could provide good results in significantly less computational time for the problem of estimating gas concentrations.

CONCLUSIONS

This work investigates Bayesian approaches to quantify the uncertainty in fitting FTIR radiometric data to models of emission from fireballs. Bayesian approaches are necessary for this problem due to the correlation in the model parameters that are used to fit the data, the low sensor spectral resolution, and to quantify the uncertainty in the fireball parameters.

One of the challenges with these approaches is the time it takes to compute the models $m_s(\nu)$. The computation is long since the FTIR model spectra have to be computed at high resolution (millions of wavenumbers) and then convolved down to the sensor wavenumbers by using the appropriate line-shape. A future step in this work is to look at the statistical narrow band (SNB) [8] approach or k-distribution theory as a method to compute model spectra more quickly. A drawback to using an approach such as SNB is that the sensor line-shape cannot be modeled and the underlying spectra are on a fixed grid that will likely differ from the sensor band center wavenumbers. A future direction is to combine the approaches so that spectral models can be computed quickly (e.g., with SNB) for many models and then computed more accurately for a fewer number of models with the full line-by-line spectral modeling used in this paper. In such a hierarchical approach, many models would be computed with SNB throughout the parameter space and then the line-by-line method would be used in regions of the parameter space that look promising.

REFERENCES

[1] Gross, K. C., 2007. "Phenomenological Model for Infrared Emissions from High-Explosive Detonation Fireballs". PhD Thesis, Air Force Institute of Technology, WPAFB, OH, September.

[2] Gross, K. C., and Perram, G. P., 2008. "The Phenomenol-

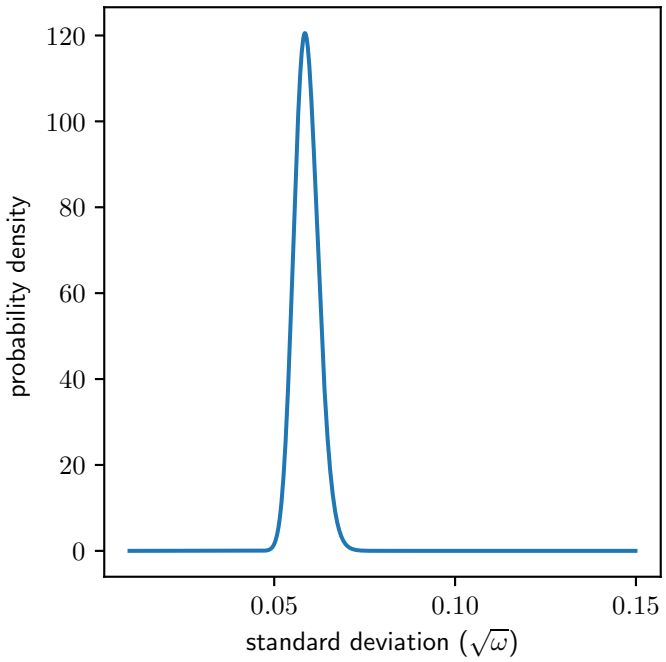

FIGURE 5. BAYESIAN CALIB. FOR $\sqrt{\omega}$

ogy of High Explosive Fireballs From Fielded Spectroscopic and Imaging Sensors for Event Classification". *Internationl Journal of High Speed Electronics and Systems,* ***18***(1), pp. 19–29.

[3] Slagle, S., 2009. "Advanced Radiometry for High Explosive Fireball Discrimination". MS Thesis, Air Force Institute of Technology, WPAFB, OH, March.

[4] Steward, B., Gross, K., and Perram, G., 2012. "Modeling midwave infrared muzzle flash spectra from unsuppressed and flash-suppressed large calibar munitions". *Infrared Physics & Technology,* ***55***, pp. 246–255.

[5] Burr, T., Fry, H., McVey, B., and et. al, 2008. "Performance of Variable Selection Methods in Regression Using Variations of the Bayesian Information Criterion". *Communications in Statistics - Simulation and Computation,* ***37***(3), May, pp. 507–520.

[6] Raftery, A., Madigan, D., and Hoeting, J., 1997. "Bayesian Model Averaging for Linear Regression Models". *Journal of the American Statistical Association,* ***92***, pp. 179–191.

[7] Neath, A., and Cavanaugh, J., 1997. "Regression and Time Series Model Selection Using Variants of the Schwarz Information Criterion". *Communications in Statistics - Theory and Models,* ***26***, pp. 559–580.

[8] Riviere, P., and Soufiani, A., 2012. "Updated band model parametes for H2O, CO2, CH4, and CO radiation at high temperature". *Internationl Journal of Heat and Mass Transfer,* ***55***, pp. 3349–3358.

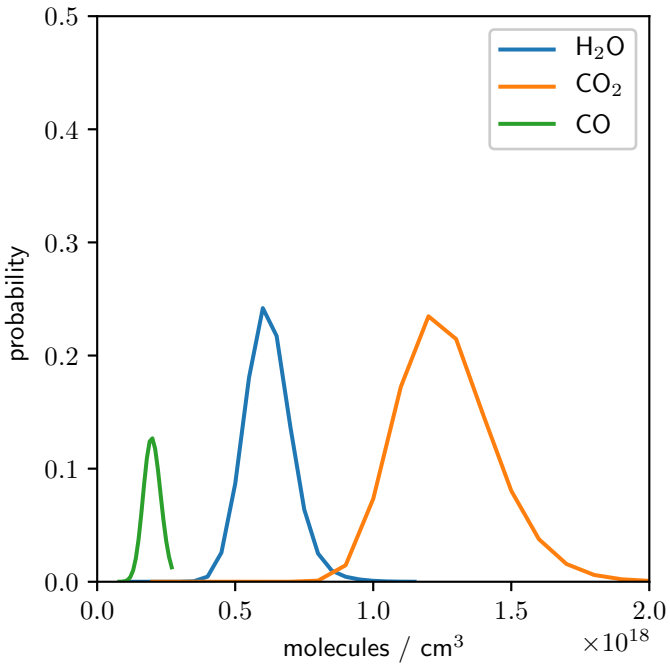

FIGURE 6. BMA RESULTS FOR GAS CONCENTRATIONS

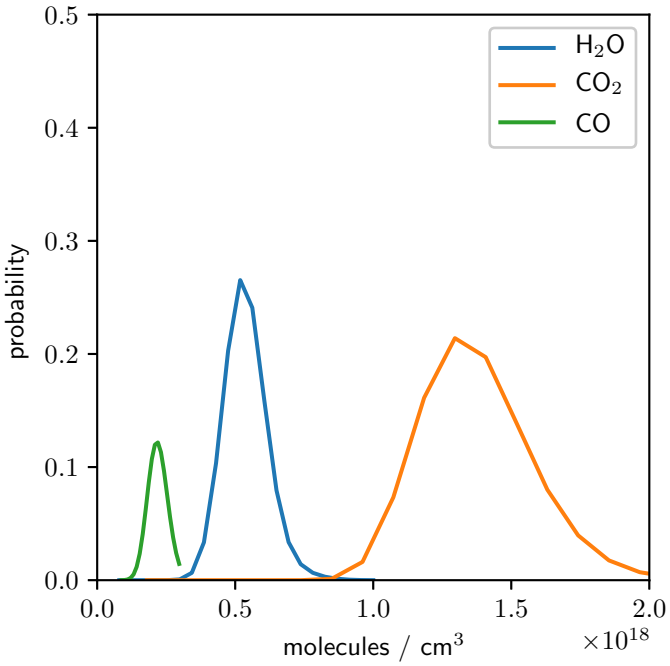

FIGURE 7. BAYESIAN CALIB. FOR GAS CONCENTRATIONS